Available online at www.sciencedirect.com
ScienceDirect
Computational Materials Science 39 (2007) 137–141
COMPUTATIONAL MATERIALS SCIENCE
www.elsevier.com/locate/commatsci

Simulations of stress–strain heterogeneities in copper thin films: Texture and substrate effects

Filip Šiška [a,*], Samuel Forest [a], Peter Gumbsch [b]

[a] *Ecole des Mines de Paris/CNRS, Centre des Matériaux/UMR 7633, BP 87, 91003 Evry, France*
[b] *IZBS, Universität Karlsruhe, Kaiserstr 12, 76131 Karlsruhe, Germany*

Received 30 September 2005; received in revised form 20 January 2006; accepted 18 February 2006

Abstract

Finite element simulations of the elastic and elastic–plastic deformation of copper thin films are performed in the presence or not of substrate. The investigated textures are {111} and {001}. In the anisotropic elastic case, {001} films are associated with more strain heterogeneities than {111} films. Strong plastic strain heterogeneities are found in {001} films. The presence of a substrate increases significantly the heterogeneity of stress–strain fields.

Keywords: Finite elements; Thin films; Polycrystals; Crystal plasticity

1. Introduction

Metal thin films are widely used in microelectronics systems [1]. Thin films are subjected to different types of loading in devices. Outstanding mechanical properties contribute to higher lifetimes in microelectronics systems. The behavior of films very often deviates from the behavior of bulk materials [1–5]. The properties of the films are related to the microstructure, texture, grain size, thickness and other parameters of the films. Some properties like toughness depend on the thickness and this is associated with size effects [2]. The origin and influence of these size effects is studied by different approaches. One of them is the finite element method within the framework of crystal plasticity [9–11].

Elastic and elasto-plastic computations of the tensile deformation of copper thin films are presented in this paper. The morphology of the film and its representation with FE mesh are described in the first part, then the suited mesh density and representative volume element size are determined. The results of elastic and elasto-plastic computation are shown focusing on stress and strain heterogeneities in the films.

2. Morphology of the grains and computational tools

2.1. Morphology, FE mesh, crystallographic texture

The computations are made with films which are represented by polycrystalline aggregates. There are two most common orientations of the grain in copper films {001} and {111} [2,6]. Usually there is only one grain through the thickness of the film and the diameter of the grain in the plane of the film is about the value of film thickness [1].

The texture is ideal: the axis {001} or {111} are exactly perpendicular to the plane of the film. The remaining in-plane orientation of the grain is random. Two extreme cases are assumed: free-standing film and film on a rigid substrate. Boundary conditions are described on the Fig. 1. The displacement component U_2 is prescribed on the lateral surfaces $X_2 = 0$ and $X_2 = L$ (L – length of the film). The existence of the substrate is modeled by the

* Corresponding author.
E-mail address: siska@mat.ensmp.fr (F. Šiška).

0927-0256/$ - see front matter © 2006 Elsevier B.V. All rights reserved.
doi:10.1016/j.commatsci.2006.02.025

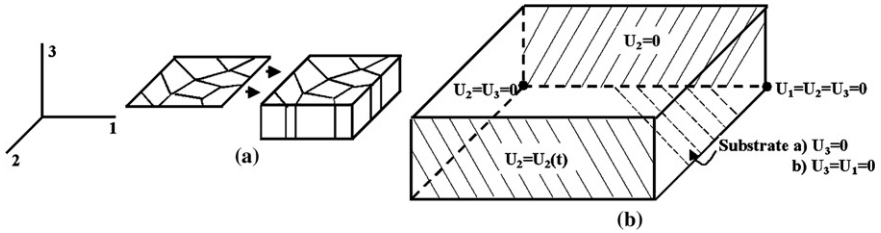

Fig. 1. (a) Extension of 2D microstructure into 3D, (b) boundary conditions for the computations.

conditions $U_3 = 0$ or $U_3 = U_1 = 0$. Code Zebulon is used for creating the polycrystalline aggregates and for all computations (*www.nwnumerics.com*). The mesh was created in two steps. First the 2D mesh was created. The grains are represented by a Voronoi mosaic, which is widely used for such simulations [11]. This 2D mesh was then simply extended in the third direction (Fig. 1). This simple extension means that all grain boundaries are exactly perpendicular to the plane of the films, which is not far from the the reality [7].

Two main issues had to be checked before starting the computations. First, the mesh density must be sufficient which requires a sufficient number of elements in one grain. The second important point is the number of grains in the films. It means the size of a representative volume element which will represent with sufficient accuracy the macroscopic behavior of the film. We present here the determination of mesh density and RVE size for elastic behaviour of copper film. Elastic parameters of copper are $C_{11} =$ 159,300 MPa, $C_{12} = 122{,}000$ MPa, $C_{44} = 81{,}000$ MPa [12]. The coefficient of anisotropy is $\alpha = 2C_{44}/(C_{11} - C_{12}) =$ 4.34.

2.2. Mesh density

This problem was solved by creating one aggregate which was meshed with four meshes with different densities: coarse – 1290 degrees of freedom per grain (dof/g), medium – 2169 dof/g, fine – 3729 dof/g and ultrafine – 6924 dof/g. A tensile test was simulated. Boundary conditions are described in Fig. 1. The global and local convergences were checked.

Global convergence: The resulting apparent Young's modulus was computed for each mesh. The global average stress in the aggregate and the Young's modulus was computed according to

$$\Sigma_{22} = \langle \sigma_{22} \rangle = \frac{1}{V} \int \sigma_{22} \mathrm{d}V, \quad E_{22} = \langle \varepsilon_{22} \rangle, \quad E_{\mathrm{app}} = \frac{\Sigma_{22}}{E_{22}}, \tag{1}$$

where E_{22} is the applied average tensile strain component.

Local convergence: In this case the values of equivalent von Mises stress along a side line of the aggregate were compared. Fig. 2 shows the results of global and local convergence. The differences between the values of different meshes are relatively small. Therefore the criterion for choosing the mesh density was the computational time and finely the medium mesh was chosen. It means that there are about 240 elements per grain.

2.3. Representative volume element

The apparent properties will coincide with the wanted effective properties only if the number of considered grains is sufficiently high [8]. For that purpose two groups of aggregates were made. The first one contained 10 different realizations of aggregates with 19–20 grains. In the second group, 20 realizations of aggregates with 47–49 grains were considered. Different realization means different shape of grains and different orientation in the plane of the film. The determination of the RVE size is illustrated in the case of elastic behavior. The simulations of the tensile response of free-standing films were made for each aggregate for both crystallographic textures. As in the previous case,

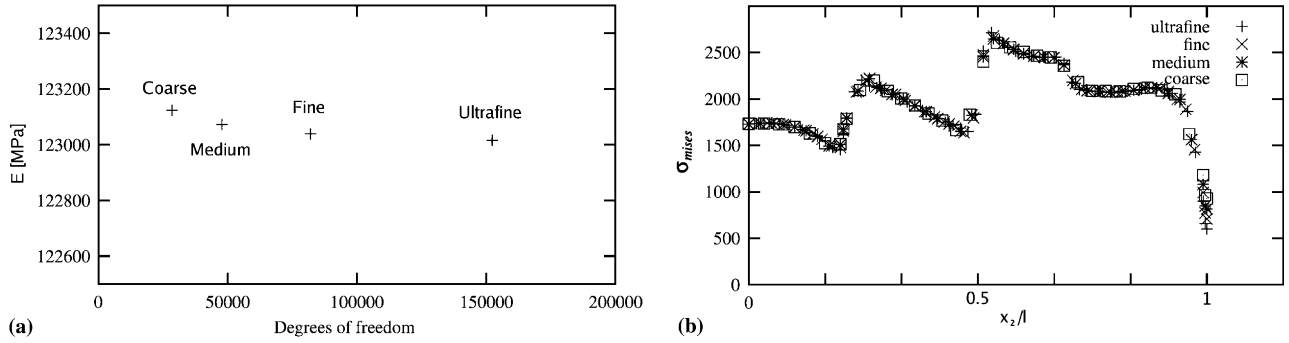

Fig. 2. Global (a) and local (b) convergence for different mesh densities.

the apparent Young's modulus was computed for each aggregate and then the mean value and dispersion for each group were estimated. We have tried to fit the following condition, which comes from the theory of sampling [8]:

$$\frac{D(E)}{\sqrt{n}\overline{E}} \leqslant 1\%, \tag{2}$$

where $D(E)$ is the dispersion, $\overline{E}$ is the mean value and n is the number of realizations. This condition is fulfilled for the aggregates with 47–49 grains. For simulations with 50 grains it is necessary to consider 20 different realizations for obtaining this precision.

3. Anisotropic elastic behaviour of thin films

The elastic anisotropy of copper is responsible for the development of stress/strain heterogeneities in films. The computations were made for aggregates with about 50 grains. Both type of textures {001}, {111} and both cases of substrate were assumed. The textures {111} is stiffer than {001}, so the resulting stresses for a given mean strain E_{22} are higher.

3.1. Texture {001}

The results for the texture {001} show that the highest stress concentrations occur at the grain boundaries. The stresses are almost constant through the thickness of the film. The constraint induced by the substrate does not have a strong influence on the distribution of the stress field in Fig. 6, because the planes {001} are symmetry planes and therefore the film remains almost perfectly flat during the deformation. But the Fig. 3a and b show that the dispersion of the stress and strain is higher in the presence of a substrate.

3.2. Texture {111}

In cubic metals, some properties in {111} planes like Young's modulus are isotropic. However a simple analytical calculation shows that it does not mean that deformation of {111}-films is homogeneous. Let us consider a single crystal loaded in tension along the direction 1 contained in a {111} plane, the direction 3 coinciding with a ⟨111⟩ direction. Mutual position of the crystal and direction of tension is described by the angle ϕ. The resulting strains are

$$\varepsilon_{11} = \sigma\left(\frac{1}{2}S_{11} + \frac{1}{2}S_{12} + \frac{1}{4}S_{44}\right), \tag{3}$$

$$\varepsilon_{22} = \sigma\left(\frac{1}{6}S_{11} + \frac{5}{6}S_{12} - \frac{1}{12}S_{44}\right), \tag{4}$$

$$\varepsilon_{33} = \sigma\left(\frac{1}{3}S_{11} + \frac{2}{3}S_{12} - \frac{1}{6}S_{44}\right), \tag{5}$$

$$\varepsilon_{12} = 0, \tag{6}$$

$$\varepsilon_{23} = \sigma\frac{\sqrt{2}\cos(3\phi)}{6}\left(S_{11} - S_{12} - \frac{1}{2}S_{44}\right), \tag{7}$$

$$\varepsilon_{13} = -\sigma\frac{\sqrt{2}\sin(3\phi)}{6}\left(S_{11} - S_{12} - \frac{1}{2}S_{44}\right), \tag{8}$$

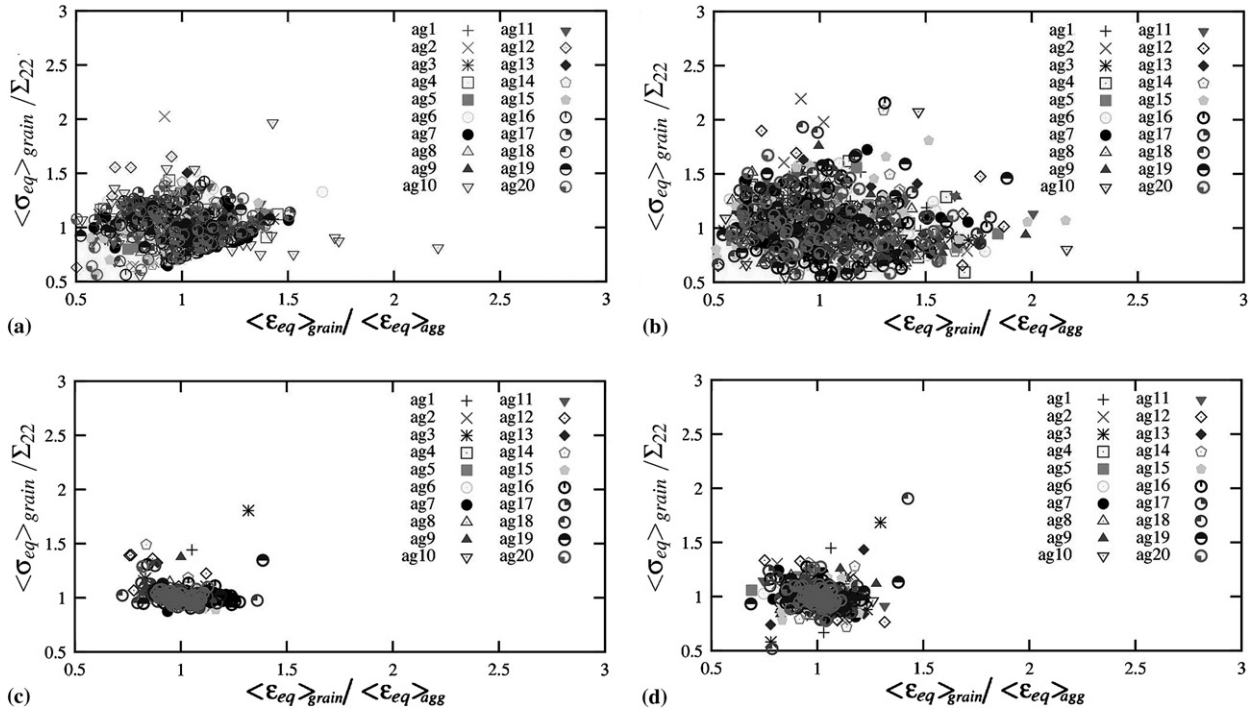

Fig. 3. Comparison of the stress and strain dispersions in aggregates (a) texture {001} without substrate, (b) texture {001} with substrate, (c) texture {111} without substrate, (d) texture {111} with substrate.

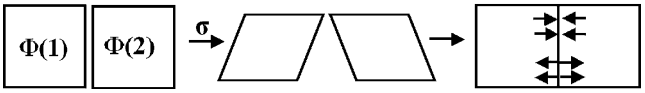

Fig. 4. Two grains with different orientation ϕ are in tension differently deformed and it causes stress concentration at the grain boundary in {1 1 1}-films.

where the S_{ij} are the cubic elastic compliances. These equations show that the diagonal part of the strain tensor is independent of angle ϕ. But out of plane shear components depend on this angle ϕ, because {1 1 1} planes are not symmetry planes for cubic crystals. Different shear strains in differently oriented grains lead to incompatibilities close to grain boundaries and the concentration of stresses and strains can be observed on these boundaries (Fig. 4). The Fig. 6c and d shows the typical results for the {1 1 1} texture. There is a larger difference between the case with and without substrate. The film does not remain flat during the deformation and this trend for curving causes additional stress concentration.

The fluctuation of stress and strain were computed and compared in the different situations. The global average values of the equivalent von Mises stress and equivalent strain were computed for each grain. The Fig. 3 shows the dispersion of the the equivalent von Mises stress and equivalent strain in aggregates, where each point represents the average value in one grain, normalized by the global mean value for the corresponding aggregate. The dispersion is much larger in the case of the texture {0 0 1}. It is due to the quasi-isotropy in the plane {1 1 1}. The substrate induces a higher dispersion of the stress than in free-standing films. The results of both boundary conditions for the rigid substrate are very similar, only the results which correspond with boundary conditions (a) (see Fig. 1(b)) are shown.

The comparison of the dispersion of the stress inside the grains in one aggregate is shown in Fig. 5. It shows the local equivalent von Mises stress in each gauss point σ_{eq} as a function of the distance from the center of the grain. This distance is normalized by the average grain size d_{av} The shape of the cluster of points shows that the dispersion is higher close to grain boundaries for the {1 1 1} texture.

4. Plastic computation

For the elasto-plastic computations, the framework of crystal plasticity is used [9–11]. The constitutive equations are:

$$F = F^e.F^p, \quad \dot{F}^p.F^{p-1} = \sum_{s=1}^{n} \dot{\gamma}^s P^s, \quad P^s = m^s \otimes n^s, \tag{9}$$

$$\tau^s = P^s : \sigma^s, \quad \dot{\gamma}^s = \left\langle \frac{|\tau^s| - r^s}{k} \right\rangle^n \operatorname{sign}\tau^s, \tag{10}$$

$$r^s = r_0 + q \sum_{r=1}^{n} h^{sr}(1 - \exp(-bv^r)). \tag{11}$$

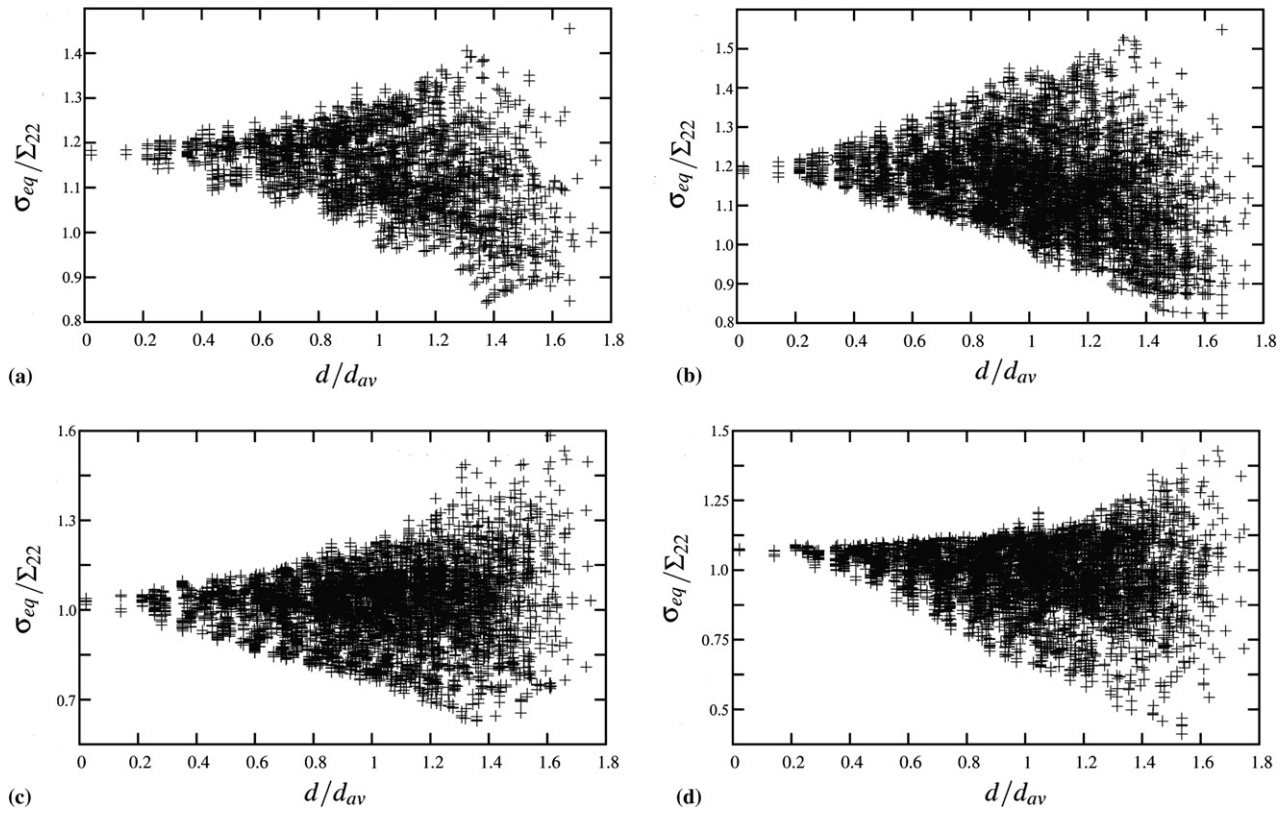

Fig. 5. Dispersion of normalized σ_{eq} as a function of normalized distance from the center of the grain (a) texture {0 0 1} without substrate, (b) texture {0 0 1} with substrate, (c) texture {1 1 1} without substrate, (d) texture {1 1 1} with substrate.

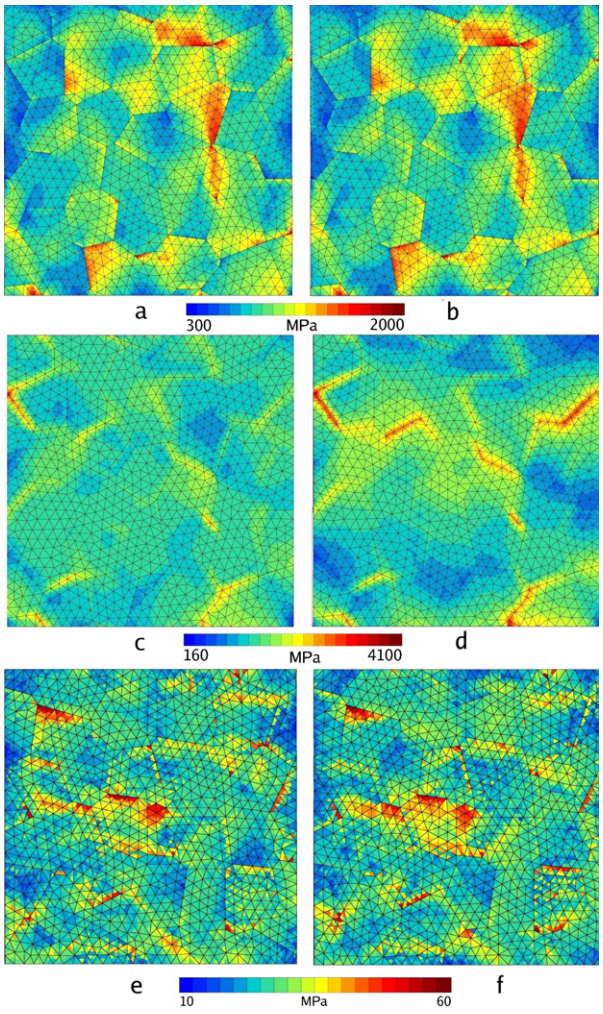

Fig. 6. Results of computations for σ_{eq}, $E_{22} = 1\%$: 1. elastic: (a) {001} without substrate, (b) {001} with substrate, (c) {111} without substrate, (d) {111} with substrate, 2. elasto-plastic: (e) {001} without substrate, (f) {001} with substrate.

The parameters K, n, r_0, q, b have been set by using of the experimental results of tensile test for single crystals of copper in different directions [12]: $K = 2$, n=15, $r_0 = 0.9$, $q = 80$, $b = 3.5$. The total deformation of the film is 1%. The Fig. 6e and f shows the values of σ_{eq} for {001} texture: (e) without substrate, (f) with substrate. Some stress concentration at the grain boundaries are visible. There is also a large heterogeneity in plastic deformation where the local values lie between 0.2% and 4.0% for global value $E_{22} = 1\%$. The dispersion of plastic deformation is larger in the presence of substrate.

5. Conclusion

The elastic and elasto-plastic behaviour of copper polycrystalline aggregate of copper with texture {001} and {111} was simulated.The strain and stress heterogeneities were compared. The main results are:

- Deformation is heterogeneous in {111} films although if the {111} plane is the plane of isotropy for Young's modulus.
- Stress and strain in texture {001} are more heterogeneous than in {111} films.
- Stress concentration is close to the grain boundaries in {111} films.
- Substrate induces larger dispersions of stress and strain. This effect is more significant in {111} texture.

Acknowledgement

This work is part of the project SizeDePen. This is the Marie Curie European research training network focusing on topic Engineering Mechanics Based on Size-Dependent Material Properties. (*www.sizedepen.de*).

References

[1] S.P. Baker, A. Kretschmann, E. Arzt, Acta Mater. 49 (2001) 2145–2160.
[2] M. Hommel, O. Kraft, Acta Mater. 49 (2001) 3935–3947.
[3] R.-M. Keller, S.P. Baker, E. Arzt, Acta Mater. 47 (1999) 415–426.
[4] S.P. Baker, R.-M. Keller-Flaig, J.B. Shu, Acta Mater. 51 (2003) 3019–3036.
[5] H. Huang, F. Spaepen, Acta Mater. 48 (2000) 3261–3269.
[6] A. Wikstrom, M. Nygards, Acta Mater. 50 (2002) 857–870.
[7] B. Okolo, P. Lamparter, U. Welzel, T. Wagner, E.J. Mittemeijer, Thin Solid Films 474 (2005) 50–63.
[8] T. Kanit, S. Forest, I. Galliet, V. Mounoury, D. Jeulin, Int. J. Solids Struct. 40 (2003) 3647–3679.
[9] G. Cailletaud, S. Forest, D. Jeulin, F. Feyel, I. Galliet, V. Mounoury, S. Quilici, Comp. Mater. Sci. 27 (2003) 351–374.
[10] F. Eberl, S. Forest, T. Wroblewsky, G. Cailletaud, J.L. Lebrun, Metall. Mater. Trans. A 33A (2002) 2825–2833.
[11] F. Barbe, L. Decker, D. Jeulin, G. Cailletaud, Int. J. Plasticity 17 (2001) 513–536.
[12] L. Meric, G. Cailletaud, M. Gasperini, Acta Metall. Mater. 42 (1994) 921–935.